

## Transition from a Linear to a Harmonic Potential in Collective Dynamics of a Multifilament Actin Bundle

Jörg Schnauß,<sup>1,\*</sup> Tom Golde,<sup>1</sup> Carsten Schuldt,<sup>1</sup> B. U. Sebastian Schmidt,<sup>1</sup> Martin Glaser,<sup>1</sup> Dan Strehle,<sup>1</sup>  
Tina Händler,<sup>1</sup> Claus Heussinger,<sup>2</sup> and Josef A. Käs<sup>1</sup>

<sup>1</sup>*Institute of Experimental Physics I, Universität Leipzig, Linnéstraße 5, 04103 Leipzig, Germany*

<sup>2</sup>*Institute for Theoretical Physics, Georg-August University of Göttingen, Friedrich-Hund Platz 1, 37077 Göttingen, Germany*

(Received 6 February 2015; revised manuscript received 25 September 2015; published 10 March 2016)

Attractive depletion forces between rodlike particles in highly crowded environments have been shown through recent modeling and experimental approaches to induce different structural and dynamic signatures depending on relative orientation between rods. For example, it has been demonstrated that the axial attraction between two parallel rods yields a linear energy potential corresponding to a constant contractile force of 0.1 pN. Here, we extend pairwise, depletion-induced interactions to a multifilament level with actin bundles, and find contractile forces up to 3 pN. Forces generated due to bundle relaxation were not constant, but displayed a harmonic potential and decayed exponentially with a mean decay time of 3.4 s. Through an analytical model, we explain these different fundamental dynamics as an emergent, collective phenomenon stemming from the additive, pairwise interactions of filaments within a bundle.

DOI: [10.1103/PhysRevLett.116.108102](https://doi.org/10.1103/PhysRevLett.116.108102)

Interactions of actin and its molecular motor myosin are known as the fundamental process for biological force generation. These interactions convert chemical energy into mechanical work by adenosine triphosphate hydrolysis [1,2]. However, we show an alternative mechanism of force generation in the absence of any molecular motors or actin accessory proteins. The system is not driven by adenosine triphosphate hydrolysis and relies solely on minimization of the free energy based on filament-filament interactions. Interactions are induced by a crowded environment in a regime well below the macromolecular content of biological cells [3].

These so-called depletion forces were originally described by spherical colloidal particles suspended in a polymeric solution [4,5]. However, this effect inherently appears in crowded solutions independent of the geometry of colloidal particles. Besides lateral particle attraction, the influence of depletion forces on axially shifted rodlike colloids has already been described by theoretical approaches [6–8]. All these approaches describe the relative shift of two rodlike particles due to the induced interaction. Arising forces are found to be constant in the axial shift since the energy gain per unit length is uniform.

Recently, Hilitski *et al.* experimentally verified these approaches by investigating the overlap of single microtubule filaments [9]. They found a constant force driving these two rods towards a maximized overlap of their excluded volumes. Additionally, force components sum up in a pairwise manner when introducing a third rod to the system [9]. Investigations of the axial attraction of two or three filaments due to depletion forces were performed with microtubules. Because of their stiffness they are appropriate to test pairwise interactions. However, microtubules cannot

be easily transferred to a multifilament system. Thus, we have chosen actin bundles formed by the depletant methyl cellulose [10–13] and illustrate that the very different dynamics of a multifilament system is a direct consequence of the additivity of various filament pairs. In this way, we extended a pairwise filament system to a multifilament scale and describe a different, emerging behavior of rodlike colloids. In contrast to microtubules, actin filaments are semiflexible underlying strong thermal fluctuations, which renders investigations of pairwise interactions challenging. Therefore, the pairwise interactions of microtubules and the multifilament interactions in actin bundles complement each other forming a comprehensive picture of axial filament attraction by depletion forces.

We used a mesoscopic approach allowing us to deflect bundles from their energetic minimum by pulling forces exerted by optical tweezers. We investigated kinetics and restoring forces arising from the relative, axial sliding of single rodlike filaments within the bundle. Observed responses did not yield a constant force—in contrast to a two filament system—but an exponential force decay. These unexpected, complex dynamics can be explained by a mathematical model that extends pairwise, linear interactions to a multifilament scale. Additionally, the model is verified by simulations. These emergent dynamics can exert forces corresponding to a regime of weak active behavior of single myosin motors [14,15].

To probe these contractions, we used two different experimental approaches. A dual-trap configuration was used to maneuver one bead while the other bead was held at a constant position. This pulling process resulted in a stretched bundle exceeding its former contour length since overlapping filaments were axially deflected from their

energetic minimum. After releasing the deflected bead from the trap, the bundle started to contract [Fig. 1(a)]. This process was recorded as an image series of the fluorescent signals (Fig. 1(b), Movie S1 [16]). A bead tracking algorithm—computed with adapted MATLAB routines provided by Pelletier *et al.* [29]—was used to transform these image series to trajectories. Following data evaluations were conducted with self-written MATLAB scripts as described previously [30]. Alternatively, an arrangement of only one bead attached to a bundle was employed. By displacing the bead, the bundle was dragged through the solution. The longitudinal viscous drag elongated the bundle [Fig. 1(c)]. Immediately after the movement was stopped bundles started to contract and fluorescent signals were recorded (Movie S2 [16]). To evaluate these experiments, a kymograph (picture series joined in one image) was used to visualize the bundle length over time [Fig. 1(d)]. Standard edge detection routines of MATLAB were employed to extract the bundle length at given times.

These methods are suitable for the investigation of dynamics of the system. However, multifilament systems involve a variety of parameters (such as molecular content, bundle thickness, filament length distributions, and more) yielding diverse starting conditions for every experiment.

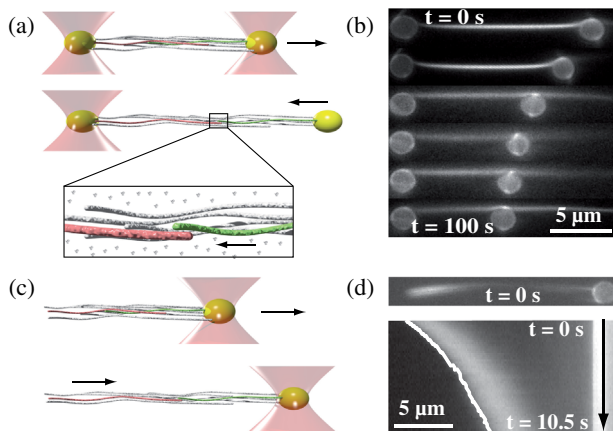


FIG. 1. (a) Optical tweezers were used to stretch bundles exceeding normal elastic deformations. After releasing one bead from the trap the bundle started to contract (Movie S1 [16]). In a stretched bundle, the overlap of excluded volumes was not maximized anymore. When the pulling force was switched off, filaments tended to maximize this overlap again and contractions appeared (magnification). A bead tracking algorithm was used to transform the recorded image series to bead trajectories, giving the bundle length between these two beads over time. (b) After the pulling process the right bead was released and the bundle relaxed to a position maximizing the overlap of the excluded volumes again. (c) The bead can be trapped and moved through the viscous solution stretching the bundle due to friction. When the movement is stopped, the bundle started to contract. (d) Displayed are the first frame of the picture series and the kymograph of a contractile actin bundle attached to one bead with detected bundle length over time.

In our experiments we tested responses of filament bundles under stress and recorded strains exceeding normal elastic deformations (up to 175 % of the initial contour length). Because of actin's rigidity these elongations can neither be attributed to thermal fluctuations of single filaments nor stretching of the filament backbone. Thus, within the pulling process filaments were pulled apart and overlapping excluded volumes of filaments were not maximized anymore. After stress release bundles started to contract. This behavior can be attributed to filaments restoring a maximal overlap of their excluded volumes.

Although previous studies revealed a constant force for pairwise overlapping filaments, the decreasing bundle length over time in our experiments is well described by an exponential decay [Fig. 2(a)]. Thus, bundle dynamics correspond to an overdamped relaxation in a harmonic free energy landscape. These dynamics arise due to the multifilament nature of probed actin bundles as described in the mathematical model below. Resulting exponential decay functions [bundle length ( $t$ ) =  $a \exp(-t/\tau) + c$ ] yield a distribution of decay times  $\tau$  showing the

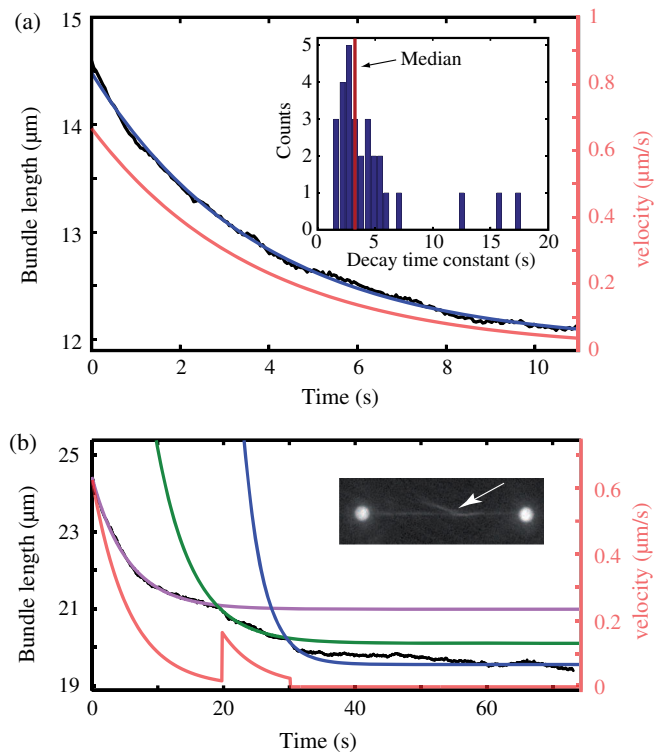


FIG. 2. (a) The recorded bundle length over time is well described by an exponential decay allowing an evaluation of the contraction velocity (red graph). Decay times (inset) of 29 different contractions are consistent with a median of 3.4 s. (b) A contracting bundle can exhibit multiple contraction events (due to a split bundle structure) described by a series of exponential decay functions with consistent decay times. The black curve displays the bundle contraction overlaid with the corresponding single exponential decay functions. The red graph is the corresponding velocity for the contractions and accelerating events.

consistency of the effect with a median of 3.4 s [Fig. 2(a), inset]. Determined exponential decays were used to calculate the velocity of contractions showing maximal speeds in the range from 0.10 to 0.65  $\mu\text{m s}^{-1}$  (Fig. S2 [16]). Resulting maximal forces were evaluated by Stokes' law and typically range from 0.5 to 3.0 pN (Fig. S2 [16]).

In three cases we observed contractions involving additional accelerating events. These rendered one single exponential decay inappropriate [Fig. 2(b)] to describe the whole contraction process. Those contractions, however, can be well described by a series of exponential decay functions. Interestingly, the decay times of these individual exponential decay functions are consistent. In general, we attribute these accelerating events to split bundle structures. A part of the bundle with originally overlapping filaments was fully detached during the stretching process. Filaments in the “main bundle” still shared excluded volumes to cause contractions. When releasing the external stress these bundles started to contract lacking the contribution of the nonoverlapping filaments. Their formerly attractive potential was not involved in the cumulative energy balance of the starting contraction. At a certain point nonoverlapping filaments came close enough to share excluded volumes with the already contracting bundle. New overlaps changed the attractive potential and accordingly the energy balance. Thus, a second or third additional internal contraction process set in and the overall contraction was accelerated again [Fig. 2(b)].

To model the results of our experiments we extend the depletion-induced interaction between filaments from individual filament pairs to a multifilament scale. Within the model a bundle is represented as a two-dimensional arrangement of  $N$  rigid rods of length  $L$ . The only degree of freedom of the rods is their relative axial shift  $x_i$  [Fig. 3].

The Hamiltonian is given by

$$H = -u \sum_{i=1}^{N-1} (L - |x_i|) - f \sum_{i=1}^{N-1} x_i, \quad (1)$$

where the first term represents the depletion-induced attraction between filaments, assumed pairwise additive, and of strength  $u$ , which has been shown to be constant in earlier studies [6–9]. The second term is the work done by the external pulling force  $f$ . The free energy  $\mathcal{F}$  and the force-extension relation  $\langle R - L \rangle = -\partial\mathcal{F}/\partial f$  can easily be calculated numerically. In the large- $N$  limit one obtains in linear response

$$\langle R - L \rangle = f \frac{N \langle x^2 \rangle}{k_B T}, \quad (2)$$

which is a consequence of the law of large numbers (similar as, for example, in the Gaussian chain model). The value  $\langle x^2 \rangle$  represents axial fluctuations of a single filament pair in the absence of force ( $f = 0$ ). Neglecting end effects, it is given by  $\langle x^2 \rangle = 2/(\beta u)^2$ , where  $\beta = 1/k_B T$ . As a result, we find the force to be proportional to the extension with a

spring constant  $k = u^2/(Nk_B T)$ . In Fig. 3(a) we numerically calculate the free energy of this model as a function of the bundle extension  $R - L$  and the number of filaments  $N$  that are arranged laterally. With two filaments in the arrangement (one pair), the free energy is a linear function of bundle extension, as expected from the definition of the model. However, this linear relation does not persist for multifilament arrangements. Already bundles with four filaments display approximately a harmonic free energy that very closely resembles the asymptotic form ( $N \rightarrow \infty$ ).

Thus, within the analytical model a combination of several linear force pairs in an additive manner yields a relation describing a harmonic potential. The origin of this transition is the addition of more and more internal degrees of freedom (in our case, the relative sliding of each individual pair) contributing an entropic term to the free energy. Extended bundles have a much smaller entropy, because the accessible configuration space for bundle conformations is highly reduced.

We note that the Hamiltonian can be extended to account for frictional forces between sliding filaments, which were reported recently [31]. In contrast to our study, Ward *et al.* employed the depletant polyethylene glycol (PEG) to bundle actin filaments, which inherently forms very dense bundled structures with a much shorter interfilament spacing [31,32]. For high PEG concentrations, the

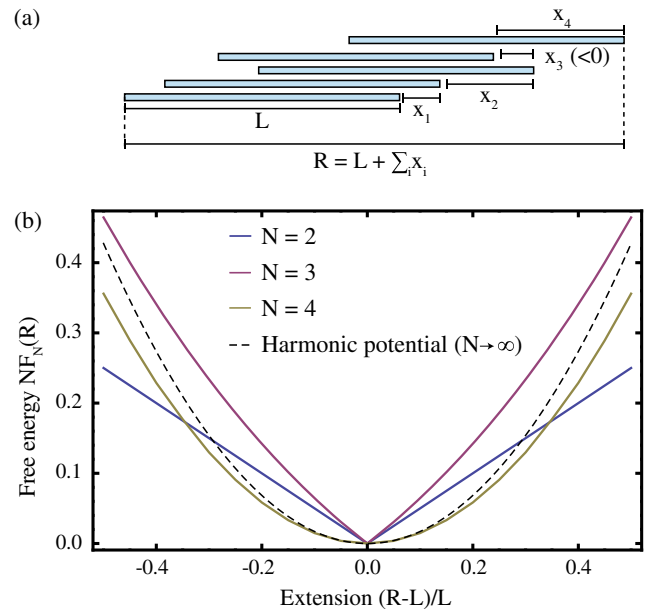


FIG. 3. (a) Schematic of the idealized 2D scenario, where forces are applied at the first ( $i = 1$ ) and at the last filament ( $i = N$ ).  $L$  denotes the unit filament length and  $R$  the length of the stretched bundle, with  $x_i$  as the displacement between two filaments. (b) Free energy  $F_N(R)$  vs end-to-end distance  $R$ . A two-filament bundle ( $N = 2$ ) has a linear energy landscape, but with only a few filaments ( $N = 4$ ) the asymptotic harmonic form (dashed) is nearly reached.

interfilament spacing can be further decreased, which can lead to high solidlike friction stalling any sliding motions [31]. However, for low PEG concentrations Ward *et al.* observed sliding of two filaments. For the multifilament case, we were not able to induce any sliding motions by optical tweezers independent of the PEG content. Thus, the high PEG concentrations necessary to form multifilament bundles impede studies of sliding dynamics. Our study relied on methyl cellulose as the depletant, which is known to form loose bundles with a large interfilament spacing, rendering interfilament friction negligible [32]. However, even by inducing interfilament friction into our mathematical model, the transition to a harmonic potential for the multifilament case is conserved if the depletion strength is larger than the friction (see Supplemental Material [16]).

While for the formulation of the theory several simplifying assumptions have been made, we expect this scenario to be generic and also useful to understand the complex experimental bundle contraction. The internal degrees of freedom in this case may also include filament bending fluctuations which are suppressed by extension [33], thus decreasing the entropy. The depletion force, in general, cannot be written as a sum over two-body contributions [34]. We test this assumption of the model by running molecular dynamics simulations where the depletant is modeled explicitly via soft spheres (see Supplemental Material [16]). The simulations and theoretical model are in excellent agreement, indicating that many-body effects for the depletion interaction in our case are indeed negligible. Although other studies revealed a constant force for pairwise overlapping filaments [6–8], we are able to show that pairwise linear, additive forces create a harmonic potential. This potential for attractive filament-filament interactions in our system supports the approach to describe actin bundle contractions by an overdamped harmonic motion. Within the frame of this model decreasing bundle lengths over time can be well described by an exponential decay. Our approach explains the springlike elastic behavior of the bundle under elongation predicting a spring constant  $k = cu^2/(k_B T)$ . The prefactor  $c \propto N_{3D}/N$  can be estimated to depend on the number of filament pairs  $N$  in the two-dimensional bundle element [Fig. 3(a)] and the number  $N_{3D}$  of these elements that are coupled in parallel. The precise value of  $c$  depends on the internal bundle structure and may vary with the experimental situation. With  $c = O(1)$  we are able to estimate a spring constant by using filament-filament interaction energies of  $30 k_B T/\mu\text{m}$  as measured previously [13]. The resulting  $k = 3.6 \text{ pN}/\mu\text{m}$  is in good agreement with the magnitudes of our data. We were not able to quantitatively compare this theoretical approach to our data any further due to experimental uncertainties. To our knowledge, there is no technique to determine the exact amount of filaments within the bundle *in situ* and values can be only estimated roughly [11]. Furthermore, packing effects within the bundle cannot be

resolved, which would be essential to extend our model from a simple two-dimensional arrangement to fully three-dimensional structures and to determine  $N_{3D}$ . In a three-dimensional model the underlying packing can have various influences. A single filament in the center of a bundle, for instance, can be displaced with few energy costs since overlapping excluded volumes can be maintained by other filaments. This deflection would yield a corresponding filament displacement at the bundle's end. To compare this case to a homogenous filament displacement within the bundle, a comprehensive three-dimensional model including packing effects has to be derived. However, the two-dimensional model is sufficient to explain the exponential force decay and corresponding differences of the dynamics. The model as well as simulations clearly show that the dynamics of a multifilament system are an emergent property of additive, pairwise, and linear force contributions.

To test influences of the contraction process to the bundle, we investigated the persistence of a bundle's contraction behavior. In that course, we deformed a single bundle multiple times and recorded its contraction behavior. For a better experimental realization, bundles attached solely to one bead were probed. Our experiments revealed a degenerating effect after consecutive expansions and contractions. As displayed in Fig. 4, later contractions display lower maximal velocities and reach a higher baseline representing an increased relaxed bundle length. We attribute this fact to potential filament annealing (two filaments concatenate) yielding a change in the energy balance [35]. For further

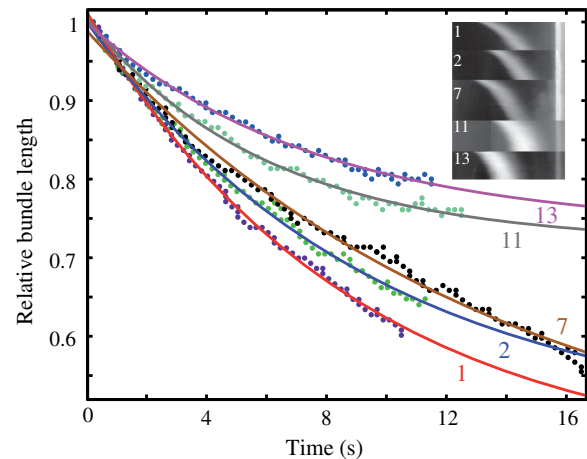


FIG. 4. Contractions show a decaying behavior when one bundle is deformed multiple times consecutively (Movie S2 [16]). Dynamic behavior becomes slower with every expansion and contraction event and the bundle relaxes to other baselines. The numbers refer to the specific contraction process. Image series were evaluated in the form of a kymograph. The relative bundle length describes the actual bundle length normalized by the maximal outstretched configuration in the corresponding experiment.

contractions these merged filaments would have to buckle and thus hinder the overall contraction process.

In conclusion, we have developed an optical tweezers based technique to investigate the contractile behavior induced by depletion forces [10] of a multifilament actin bundle. In comparison to previous theoretical as well as experimental studies [6–9] we found a fundamentally different dynamic behavior. These earlier studies described that a relative, axial sliding of single rodlike filaments induced by depletion forces leads to a constant force. Dynamics of contractions would then proceed with a constant velocity, at odds with our findings of an exponentially decreasing velocity. We are able to describe this behavior as an emergent phenomenon of rodlike colloids in an actin bundle when taking pairwise interactions to a multifilament scale. To further understand the results of our experiments we modeled the bundle as a simple two-dimensional arrangement of  $N - 1$  laterally stacked pairs of rigid filaments. The arising harmonic potential and accordingly the exponential force decay were verified by simulations as well as for the case of interfilament friction. To measure absolute force values, different techniques have to be applied as used by Hilitski *et al.* and Ward *et al.* [9,31]. These methods, however, hardly allow evaluations of dynamics. Additionally, our employed protocols are especially optimized to form large bundle structures. The investigation of two interacting actin filaments in a crowded environment requires various adjustments of the experimental protocols. In our systems, the transition from single filaments to bundles due to crowding effects is rather sharp [10,32]. Thus, if the interaction is strong enough to cause attraction, almost every filament is grouped in a bundled structure rendering experiments with a controlled number of filaments impossible. However, experiments in a two or three filament system have been already achieved illustrating the pairwise additive contributions of filaments if the sliding motions are not stalled by frictional forces [9,31]. Based on the previous findings, we extended these studies to the multifilament case yielding very different dynamics.

Molecular crowding effects represent a fundamental physical interaction, which cannot be switched off even in active systems such as cells. The cytoplasm itself is a dense environment filled with macromolecules [3,32]. In the experiments presented here the amount of macromolecules is well below the macromolecular content of a cell emphasizing the biological relevance (see Supplemental Material [16]). Additionally, kinetics and force generation are in a regime of active processes but without the need to convert chemical energy into mechanical work [1,15,36–39].

This work was supported by the DFG via the graduate school “Building with Molecules and Nano-Objects” (GSC 185) and the DFG Forschergruppe (FOR 877). We gratefully acknowledge funding by the European Social Fund

(ESF) and the Free State of Saxony. C. H. acknowledges the support of the DFG via the Emmy Noether Fellowship He 6322/1-1 as well as via the collaborative research center SFB 937, project A16.

\*joerg.schnauss@uni-leipzig.de

- [1] H. F. Lodish, *Molecular Cell Biology*, 4th ed. (W. H. Freeman, New York, 2000).
- [2] F. Huber, J. Schnauß, S. Rönicke, P. Rauch, K. Müller, C. Fütterer, and J. Käs, Emergent complexity of the cytoskeleton: from single filaments to tissue, *Adv. Phys.* **62**, 1 (2013).
- [3] R. Ellis, Macromolecular crowding: obvious but underappreciated, *Trends Biochem. Sci.* **26**, 597 (2001).
- [4] S. Asakura and F. Oosawa, Interaction between particles suspended in solutions of macromolecules, *J. Polym. Sci.* **33**, 183 (1958).
- [5] S. Asakura and F. Oosawa, On interaction between two bodies immersed in a solution of macromolecules, *J. Chem. Phys.* **22**, 1255 (1954).
- [6] M. Kinoshita, Interaction between big bodies with high asphericity immersed in small spheres, *Chem. Phys. Lett.* **387**, 47 (2004).
- [7] W. Li and H. R. Ma, Depletion interactions between two spherocylinders, *Eur. Phys. J. E* **16**, 225 (2005).
- [8] J. Galanis, R. Nossal, and D. Harries, Depletion forces drive polymer-like self-assembly in vibrofluidized granular materials, *Soft Matter* **6**, 1026 (2010).
- [9] F. Hilitski, A. R. Ward, L. Cajamarca, M. F. Hagan, G. M. Grason, and Z. Dogic, Measuring Cohesion between Macromolecular Filaments One Pair at a Time: Depletion-Induced Microtubule Bundling, *Phys. Rev. Lett.* **114**, 138102 (2015).
- [10] M. Hosek and J. Tang, Polymer-induced bundling of F actin and the depletion, *Phys. Rev. E* **69**, 051907 (2004).
- [11] D. Strehle, J. Schnauß, C. Heussinger, J. Alvarado, M. Bathe, J. Käs, and B. Gentry, Transiently crosslinked F-actin bundles, *Eur. Biophys. J.* **40**, 93 (2011).
- [12] A. W. C. Lau, A. Prasad, and Z. Dogic, Condensation of isolated semi-flexible filaments driven by depletion interactions, *Europhys. Lett.* **87**, 48006 (2009).
- [13] M. Streichfuss, F. Erbs, K. Uhrig, R. Kurre, A. E. -M. Clemen, C. H. J. Bohm, T. Haraszti, and J. P. Spatz, Measuring forces between two single actin filaments during bundle formation, *Nano Lett.* **11**, 3676 (2011).
- [14] K. Carvalho, F.-C. Tsai, E. Lees, R. Voituriez, G. H. Koenderink, and C. Sykes, Cell-sized liposomes reveal how actomyosin cortical tension drives shape change, *Proc. Natl. Acad. Sci. U.S.A.* **110**, 16456 (2013).
- [15] A. E.-M. Clemen, M. Vilfan, J. Jaud, J. Zhang, M. Bärmann, and M. Rief, Force-dependent stepping kinetics of myosin-V, *Biophys. J.* **88**, 4402 (2005).
- [16] See Supplemental Material at <http://link.aps.org/supplemental/10.1103/PhysRevLett.116.108102>, which includes Refs. [17–21], for more details on materials and methods as well as Refs. [22–28] for a detailed biological background.

- [17] B. Gentry, D. Smith, and J. Käs, Buckling-induced zebra stripe patterns in nematic F-actin, *Phys. Rev. E* **79**, 031916 (2009).
- [18] D. Koch, T. Betz, A. Ehrlicher, M. Gogler, B. Stuhmann, J. Kas, K. Dholakia, and G. C. Spalding, Optical control of neuronal growth, in *Optical Science and Technology: Proceedings of the SPIE 49th Annual Meeting* (SPIE, Denver, CO, USA, 2004), pp. 428–436.
- [19] S. F. Tolić-Nørrelykke, E. Schäffer, J. Howard, F. S. Pavone, F. Jülicher, and H. Flyvbjerg, Calibration of optical tweezers with positional detection in the back focal plane, *Rev. Sci. Instrum.* **77**, 103101 (2006).
- [20] Q. Zhang and I. Couloigner, Accurate centerline detection and line width estimation of thick lines using the radon transform, *IEEE Trans. Image Process.* **16**, 310 (2007).
- [21] J. Schnauß, M. Glaser, C. Schuldt, T. Golde, T. Händler, B. U. S. Schmidt, S. Diez, and J. Käs, Motor-free force generation in biological systems, *Diffusion Fundam.* **23**, 1 (2015).
- [22] M. R. Stachowiak, P. M. McCall, T. Thoresen, H. E. Balcioglu, L. Kasiewicz, M. L. Gardel, and B. O’Shaughnessy, Self-organization of myosin II in reconstituted actomyosin bundles, *Biophys. J.* **103**, 1265 (2012).
- [23] M. L. Gardel, F. Nakamura, J. H. Hartwig, J. C. Crocker, T. P. Stossel, and D. A. Weitz, Prestressed F-actin networks cross-linked by hinged filamins replicate mechanical properties of cells, *Proc. Natl. Acad. Sci. U.S.A.* **103**, 1762 (2006).
- [24] S. Romero, A. Quatela, T. Bornschlogl, S. Guadagnini, P. Bassereau, and G. T. Van Nhieu, Filopodium retraction is controlled by adhesion to its tip, *J. Cell Sci.* **125**, 4999 (2012).
- [25] T. Bornschlöggl, S. Romero, C. L. Vestergaard, J.-F. Joanny, G. T. Van Nhieu, and P. Bassereau, Filopodial retraction force is generated by cortical actin dynamics and controlled by reversible tethering at the tip, *Proc. Natl. Acad. Sci. U.S.A.* **110**, 18928 (2013).
- [26] D. Vignjevic, S.-i. Kojima, Y. Aratyn, O. Danciu, T. Svitkina, and G. G. Borisy, Role of fascin in filopodial protrusion, *J. Cell Biol.* **174**, 863 (2006).
- [27] Y. Yamakita, S. Ono, F. Matsumura, and S. Yamashiro, Phosphorylation of human fascin inhibits its actin binding and bundling activities, *J. Biol. Chem.* **271**, 12632 (1996).
- [28] S. Ono, Y. Yamakita, S. Yamashiro, P. T. Matsudaira, J. R. Gnarr, T. Obinata, and F. Matsumura, Identification of an actin binding region and a protein kinase C phosphorylation site on human fascin, *J. Biol. Chem.* **272**, 2527 (1997).
- [29] V. Pelletier, N. Gal, P. Fournier, and M. Kilfoil, Micro-rheology of Microtubule Solutions and Actin-Microtubule Composite Networks, *Phys. Rev. Lett.* **102**, 188303 (2009).
- [30] T. Golde, C. Schuldt, J. Schnauß, D. Strehle, M. Glaser, and J. Käs, Fluorescent beads disintegrate actin networks, *Phys. Rev. E* **88**, 044601 (2013).
- [31] A. Ward, F. Hilitiski, W. Schwenger, D. Welch, A. W. C. Lau, V. Vitelli, L. Mahadevan, and Z. Dogic, Solid friction between soft filaments, *Nat. Mater.* **14**, 583 (2015).
- [32] F. Huber, D. Strehle, J. Schnauß, and J. Käs, Formation of regularly spaced networks as a general feature of actin bundle condensation by entropic forces, *New J. Phys.* **17**, 043029 (2015).
- [33] F. C. MacKintosh, J. Käs, and P. Janmey, Elasticity of Semiflexible Biopolymer Networks, *Phys. Rev. Lett.* **75**, 4425 (1995).
- [34] M. Dijkstra and R. van Roij, Entropic Wetting and Many-Body Induced Layering in a Model Colloid-Polymer Mixture, *Phys. Rev. Lett.* **89**, 208303 (2002).
- [35] E. Andrianantoandro, L. Blanchoin, D. Sept, J. McCammon, and T. D. Pollard, Kinetic mechanism of end-to-end annealing of actin filaments, *J. Mol. Biol.* **312**, 721 (2001).
- [36] J. T. Finer, R. M. Simmons, and J. A. Spudich, Single myosin molecule mechanics: piconewton forces and nanometer steps, *Nature* **368**, 113 (1994).
- [37] S. J. Kron and J. A. Spudich, Fluorescent actin filaments move on myosin fixed to a glass surface, *Proc. Natl. Acad. Sci. U.S.A.* **83**, 6272 (1986).
- [38] J. M. Scholey, *Motility Assays for Motor Proteins*, Methods in Cell Biology Vol. 39 (Academic Press, San Diego, 1993).
- [39] Z. Lansky, M. Braun, A. Lüdecke, M. Schlierf, P. R. ten Wolde, M. E. Janson, and S. Diez, Diffusible cross-linkers generate directed forces in microtubule networks, *Cell* **160**, 1159 (2015).